Dual mechanisms of action of the 5-benzylidene-hydantoin UPR1024 on lung cancer cell lines

Andrea Cavazzoni,[1] Roberta R. Alfieri,[1] Caterina Carmi,[2] Valentina Zuliani,[2] Maricla Galetti,[1] Claudia Fumarola,[1] Raffaele Frazzi,[1] Mara Bonelli,[1] Fabrizio Bordi,[2] Alessio Lodola,[2] Marco Mor,[2] and Pier Giorgio Petronini[1]

[1]Department of Experimental Medicine and [2]Pharmaceutical Department, University of Parma, Parma, Italy

Abstract

In this study, we examined the mechanism of action of the novel epidermal growth factor receptor (EGFR) tyrosine kinase inhibitor 5-benzylidene-hydantoin UPR1024, whose structure was designed to interact at the ATP-binding site of EGFR. The compound had antiproliferative and proapoptotic effects when tested on the non–small cell lung cancer cell line A549. The growth inhibitory effect was associated with an accumulation of the cells in the S phase of the cell cycle. Moreover, UPR1024 induced significant level of DNA strand breaks associated with increased expression of p53 and $p21^{WAF1}$ proteins, suggesting an additive mechanism of action. The presence of wild-type p53 improved the drug efficacy, although the effect was also detectable in p53 null cells. We also noted apoptotic cell death after treatment with UPR1024 at concentrations above 10 μmol/L for >24 h, with involvement of both the extrinsic and intrinsic pathways. The present data show that UPR1024 may be considered a combimolecule capable of both blocking EGFR tyrosine kinase activity and inducing genomic DNA damage. UPR1024 or its derivatives might serve as a basis for development of drugs for the treatment of lung cancer in patients resistant to classic tyrosine kinase inhibitors. [Mol Cancer Ther 2008;7(2):361–70]

Received 7/17/07; revised 11/29/07; accepted 12/28/07.

Grant support: Regione Emilia Romagna, Associazione Chiara Tassoni (Parma, Italy), A.VO.PRO.RI.T. (Parma, Italy), and Associazione Davide Rodella (Montichiari, Italy).

The costs of publication of this article were defrayed in part by the payment of page charges. This article must therefore be hereby marked *advertisement* in accordance with 18 U.S.C. Section 1734 solely to indicate this fact.

Requests for reprints: Roberta R. Alfieri, Department of Experimental Medicine, University of Parma, Via Volturno 39 43100 Parma, Italy. Phone: 39-521-033766; Fax: 39-521-033742.
E-mail: roberta.alfieri@unipr.it

doi:10.1158/1535-7163.MCT-07-0477

Introduction

Lung cancer is the leading cause of death from malignant disease in the developed world, but only a minority of patients is eligible for radical treatment with curative intent. The availability of new cytotoxic drugs has led to incremental improvements, but a paradigm shift is required to make a significant effect on the poor prognosis for most patients. Due to major advances in cancer biology, many potential therapeutic targets have been identified. Most of these targets are components of signaling pathways or metabolic processes contributing to one of the hallmarks of the cancer phenotype (1).

One of these targets is the epidermal growth factor (EGF) receptor (EGFR). EGFR (ErbB1, HER1) is the prototypic member of the ErbB family of receptor tyrosine kinase, which also includes ErbB2-4 (HER2-4). Upon specific binding of EGF-like ligands to the extracellular domain, ErbB receptors dimerize either as homodimers or as heterodimers. After this dimerization, the receptor undergoes autophosphorylation at specific tyrosine residues within the intracellular domain. These phosphorylated tyrosines serve as docking sites for adapter molecules, such as growth factor receptor binding protein 2 and the p85 subunit of phosphoinositide 3-kinase, which activate a complex network of downstream signaling pathways. These pathways, including the Ras/mitogen-activated protein kinase and Akt/mTOR kinase cascades, in turn regulate transcription factors and other proteins involved in cell proliferation, survival, motility, and differentiation (2).

The overexpression of EGFR has been well documented in a variety of human tumors, including non–small cell lung cancer (NSCLC; ref. 3), and has been associated with poor prognosis and worse clinical outcome (4).

The 4-aniloquinazolines gefitinib (Iressa) and erlotinib (Tarceva) are the two most important anticancer drugs developed to target the EGFR tyrosine kinase activity and are used in the treatment of NSCLC (5).

However, tumor cells often acquire resistance to EGFR inhibitors through several different mechanisms. Certain mutations in the *EGFR* gene (T790M mutation; refs. 6, 7), other mechanisms, such as drug efflux or protein binding, or additional oncogenic changes downstream of the receptor have been associated with resistance to EGFR-targeting drugs (8, 9).

New EGFR tyrosine kinase inhibitors, structurally different from 4-anilinoquinazolines having additional mechanisms of cytotoxicity, need to be designed to circumvent acquired resistance to gefitinib and erlotinib therapy.

On the other hand, several studies have shown that in combination with radiation (10) or classic cytotoxic drugs (11, 12), gefitinib provided synergistic, antiproliferative, and proapoptotic actions.

We have recently shown that hydantoin derivatives designed to interact at the ATP site of EGFR inhibited the EGFR kinase activity and exerted an antiproliferative effect on the A431 cell line overexpressing EGFR (13). Among a panel of these compounds, the one originally termed 2e and now called UPR1024 showed the highest potency. UPR1024 belongs to a new class of EGFR inhibitors characterized by a hydantoin nucleus and a 5-benzylidene substituent having a double bond conjugated with a carbonyl group on the hydantoin ring.

In this study, we further investigated the effects of UPR1024 on a panel of NSCLC cell lines showing a wide range of sensitivity to gefitinib. The compound induced a significant inhibition of cell proliferation with a preferential accumulation of the cells in the S phase of the cell cycle. Apoptosis was also detectable in cells exposed to the drug as indicated by an increase in the sub-G_1 cell population, release of cytochrome *c* from mitochondria and activation of caspases 3, 8, and 9. Moreover, we found that UPR1024, a drug designed to act as tyrosine kinase inhibitor, had a genotoxic effect suggesting an additive mechanism of action. The presence of wild-type p53 improved drug efficacy, although the effect was also detectable in p53 null cells.

Overall our results suggest that UPR1024, a 1,5-disubstituted hydantoin, possesses chemical properties that confer multiple mechanisms of action and can be considered a novel combi-molecule capable of both blocking EGFR tyrosine kinase activity and inducing genomic DNA damage.

Materials and Methods

Cell Culture

The human NSCLC cell lines A549, H460, and H1299 were cultured in RPMI 1640; Calu-3 and Lx-1 were cultured in DMEM with 1 mmol/L sodium pyruvate and 0.1 mmol/L nonessential amino acids; SKLU-1 was cultured in MEM supplemented with 1 mmol/L sodium pyruvate and 0.1 mmol/L nonessential amino acids. All media were supplemented with 2 mmol/L glutamine, 10% fetal bovine serum. Cell lines were from the American Type Culture Collection and maintained under standard cell culture conditions at 37°C in a water-saturated atmosphere of 5% CO_2 in air.

Inducible p53 transfectans of cell line Calu-1 were generated from the NSCLC Calu-1 cell line as previously described (14). These stable clones, conditionally expressing the p53 gene from the Ponasterone A–inducible promoter, were maintained in RPMI 1640 in the presence of 50 μg/mL zeocin and 400 μg/mL G418.

Drug Treatment

UPR1024 was synthesized in the Pharmaceutical Department of Parma University as described elsewhere (13). In all assays, the drug was dissolved in DMSO immediately before the addition to cell cultures. The concentration of DMSO never exceeded 0.1% (v/v) and equal amounts of the solvent were added to control cells. Gefitinib was synthesized as previously reported (13).

Antibodies and Reagents

Media were from Euroclone; fetal bovine serum were purchased from Life Technologies-Bethesda Research Laboratories. Monoclonal anti–cytochrome *c* (7H8), monoclonal anti-p53 (DO-1), monoclonal anti-$p21^{WAF1}$ antibodies were obtained from Santa Cruz Biotechnology. Monoclonal anti–caspase-8 (1C12), polyclonal anti–caspase-9, polyclonal anti–caspase-3, monoclonal anti-EGFR, polyclonal anti–phospho-EGFR (Tyr^{1068}) antibodies were from Cell Signaling Technology. Monoclonal anti-actin (AC-40) antibody was from Sigma Aldrich. Horseradish peroxidase–conjugated secondary antibodies and the enhanced chemiluminescence system were from Millipore. Reagents for electrophoresis and blotting analysis were obtained from BIO-RAD Laboratories. Caspase-8 inhibitor z-IETD-FMK was purchased from Enzyme Systems Products.

Western Blot Analysis

Procedures for protein extraction, solubilization, and protein analysis by one-dimensional PAGE are described elsewhere (15). Briefly, cells were lysed, and protein concentration was determined by the dye-binding method (Bio-Rad) with bovine serum albumin as standard (16). Proteins (50–100 μg) from lysates were resolved by 5% to 15% SDS-PAGE and transferred to nitrocellulose membranes. Cytosolic and mitochondrial fractions were generated using a digitonin-based subcellular fractionation technique (17) as previously described (18). Equal volumes of cytosolic and mitochondrial fractions were resolved by SDS-PAGE and transferred to nitrocellulose membranes. The membranes were then incubated with primary antibody, washed, and then incubated with horseradish peroxidase anti-mouse or horseradish peroxidase anti-rabbit antibodies. Immunoreactive bands were visualized using an enhanced chemiluminescence system.

Autophosphorylation Assay

Inhibition of EGFR autophosphorylation in A549 cells was determined using a specific anti-phosphotyrosine antibody by Western blot analysis. Briefly, serum-starved cells were preincubated for 1 h with the indicated concentrations of UPR1024 before stimulation with 0.1 μg/mL EGF for 5 min. Equal amounts of cell lysates were analyzed by Western blotting using anti–phosphorylated EGFR (Tyr^{1068}) antibody. Membranes were stripped and reprobed with anti-EGFR antibody.

Determination of Cell Growth and Cell Cycle Analysis

Cell growth and survival were evaluated by cell counting, clonogenic assay, and 3-(4,5-dimethylthiazol-2-yl)-2,5-diphenyltetrazolium bromide assay. Briefly, cells were detached from the plates by trypsinization and counted in a Burker hemocytometer by trypan blue exclusion.

Colony formation by viable cells was determined by seeding them at a density of 400 cells per dish. After 10 days of incubation, colonies were fixed with 95% ethanol, stained with 0.1% crystal violet and counted. Colonies containing at least 50 cells were scored, and all data on viability are given as percentage versus untreated control.

Cell viability was also assessed by tetrazolium dye [3-(4,5-dimethylthiazol-2-yl)-2,5-diphenyltetrazolium bromide; Sigma] assay as previously described (15).

Distribution of the cells in the cell cycle was determined by propidium iodide staining and flow cytometry analysis (EPICS XL-MCL cytometer; Beckman Coulter). Cells (5×10^5) were harvested, washed in PBS, fixed in cold 70% ethanol, and then stained with 40 μg/mL propidium iodide while treating with RNase. Analysis was done with a Beckman Coulter EPICS XL-MCL cytometer (Beckman Coulter). Cell cycle distributions were analyzed by Multi-Cycle DNA Content and Cell Cycle Analysis Software (Phoenix Flow Systems, Inc.) as previously described (15, 18).

Detection of Apoptosis

Apoptosis was assessed by (*a*) morphology on stained (Hoechst 33342, propidium iodide) or unstained cells using light, phase contrast, and fluorescence microscopy; (*b*) analysis of phosphatidylserine exposure on the cell surface by the Annexin V–FITC assay [Bender MedSystems; briefly, 2.5×10^5 cells were harvested, washed with PBS, incubated with Annexin V–FITC and propidium iodide according to the supplier's protocol, and analyzed by flow cytometry, and data were collected using logarithmic amplification of both the FL1 (FITC) and FL3 (propidium iodide) channels and quantitated by quadrant analysis of coordinate dot plots]; (*c*) quantitative analysis of hypodiploid sub-G_1 cells by flow cytometry done after the procedure described for cell cycle analysis; (*d*) activity of caspase-3 by a colorimetric assay (Caspase Colorimetric Assay kit, MBL International Corp.) and inhibition by specific tetrapeptides (z-IETD-FMK for caspase-8); (*e*) activation of caspase-3, caspase-8, and caspase-9 (detection of cleavage products) and release of cytochrome *c* by Western Blotting procedure as previously described (18); and (*f*) dissipation of mitochondrial membrane potential by the MitoCapture Assay kit (MBL) according to published procedures (19).

Fast Halo Assay

The fast halo assay was carried out as previously described (20). Briefly, after drug treatment, cells were resuspended at 4×10^4/100 μL in ice-cold PBS containing 5 mmol/L EDTA: this cell suspension was diluted with an equal volume of 2% low-melting agarose in PBS and immediately sandwiched between an agarose-coated slide and a coverslip. After complete gelling on ice, the coverslips were removed and the slides were immersed in 0.3 mol/L NaOH for 15 min at room temperature. Ethidium bromide (10 μg/mL) was directly added during the last 5 min of incubation. The slides were then washed and destained for 5 min in distilled water.

The ethidium bromide–labeled DNA images were acquired using a Digital Net Camera (DN100, Nikon Corporation) and processed with image analysis software (Scion Image). The slides were numerically coded before

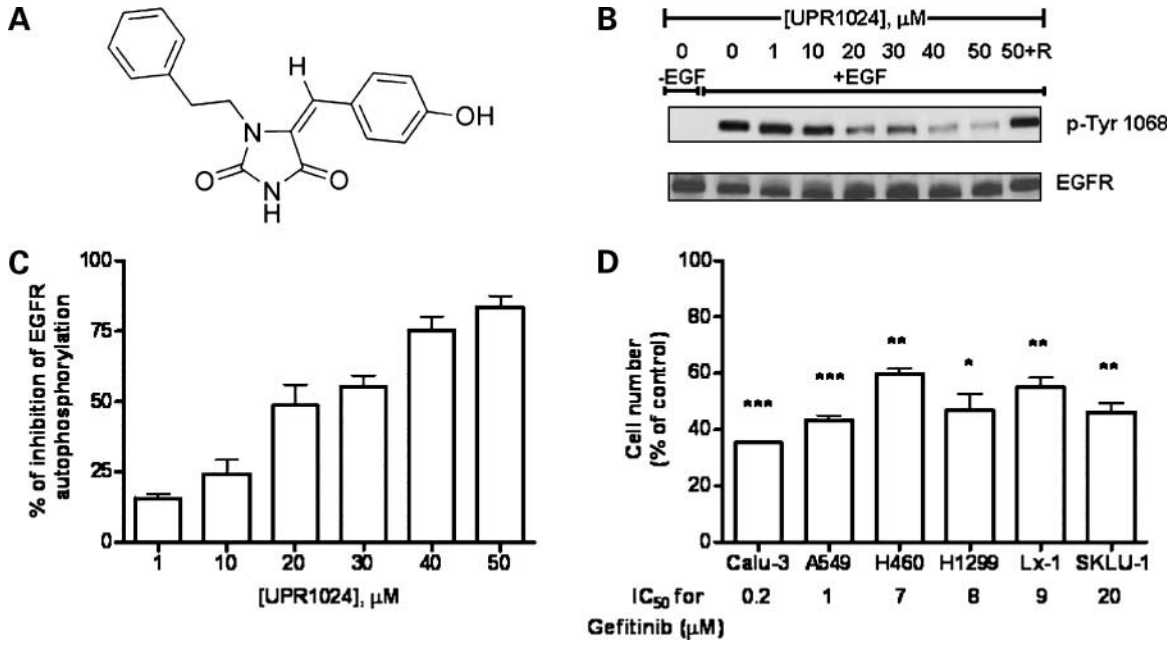

Figure 1. Structure of UPR1024 and effect of UPR1024 on EGFR autophosphorylation and cell proliferation. **A,** chemical structure of UPR1024. **B,** A549 cells were serum starved for 16 h and then preincubated for 1 h with the indicated concentration of UPR1024 before stimulation with 0.1 μg/mL EGF for 5 min. A duplicate sample was treated with 50 μmol/L UPR1024 for 1 h and stimulated with EGF after 8 h (recovery phase) in drug-free medium (50 + R). Western blot analysis was done by using monoclonal antibodies directed to p-Tyr^{1068} and to EGFR. **C,** the immunoreactive spots at each point were quantified by densitometric analysis, ratios of phosphotyrosine/total EGFR were calculated, and values are expressed as percentage of inhibition versus control. **D,** cell number was determined by cell counting in six human NSCLC cell lines exposed for 72 h to 20 μmol/L UPR1024. Results are presented as percentage of viable cells versus untreated control. The IC_{50} for growth inhibition by gefitinib, evaluated by 3-(4,5-dimethylthiazol-2-yl)-2,5-diphenyltetrazolium bromide assay, are shown. *Columns,* mean of three separate experiments; *bars,* SD (**C** and **D**). *, $P < 0.05$; **, $P < 0.01$; ***, $P < 0.001$ versus 100; $n = 3$.

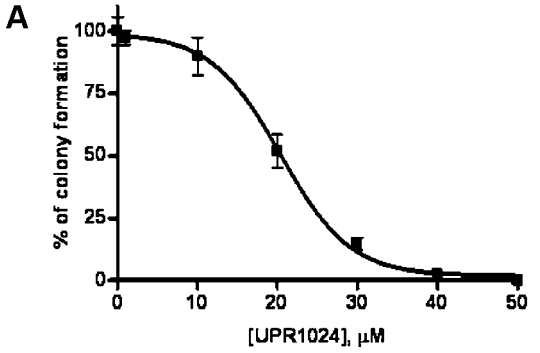

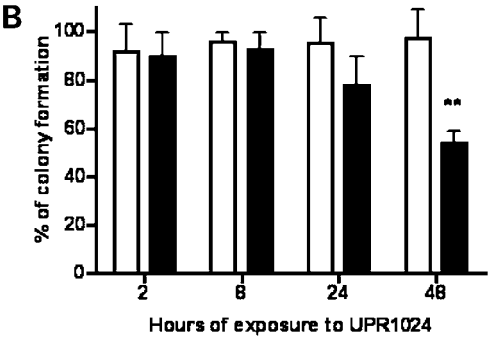

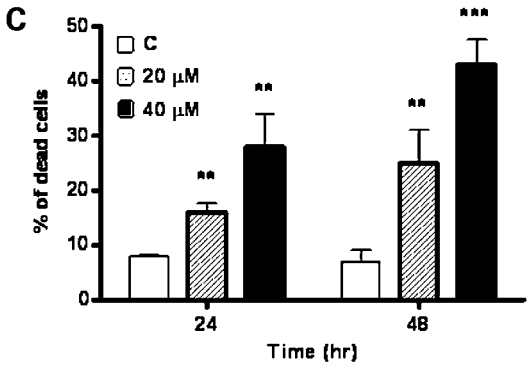

D

		subG$_1$	*G*$_0$/*G*$_1$	*S*	*G*$_2$/*M*
	C	7.3±1.2	58.0±6.0	34.0±2.5	8.3±3.5
24 hr	20 μM	12.3±4.0	46.7±4.0	* 42.3±3.1	8.0±0.6
	40 μM	* 26.0±6.9	** 27.7±3.2	*** 65.0±3.5	7.3±0.6
	C	7.0±1.7	62.0±2.1	31.0±2.0	6.7±0.6
48 hr	20 μM	** 22.0±4.0	** 48.3±2.1	** 43.3±1.5	* 8.3±0.6
	40 μM	*** 46.3±3.8	*** 16.3±4.5	*** 63.3±1.2	*** 20.3±4.7

Figure 2. Effect of UPR1024 on A549 cell proliferation, cell death, and cell cycle distribution. **A,** cells were continuously exposed to the indicated concentration of UPR1024 or transiently exposed (**B**) to 20 (*empty columns*) or 40 μmol/L (*filled columns*) UPR1024 for the indicated period of time, after which they were allowed to recover in drug-free medium. The ability of individual cells to form >50 cell colonies was assessed after 10 d. **C,** A549 cells were treated with the indicated concentrations of UPR1024 for 24 or 48 h and then analyzed by flow cytometry with Annexin V – FITC/propidium iodide staining to assess cell death. **D,** A549 cells were incubated in the absence or in the presence of 20 or 40 μmol/L UPR1024 and, at the indicated time intervals, were stained with propidium iodide and analyzed by flow cytometry for cell cycle – phase distribution and apoptotic sub-G_1 peak detection. Percentages of sub-G_1 cells and of cells residing in each cycle phase are reported in the table. *Columns,* mean values of three independent measurements; *bars,* SD. *, $P < 0.05$; **, $P < 0.01$; ***, $P < 0.001$ versus 100 (**B**) or versus control (**C** and **D**); $n = 3$.

reading to minimize operator bias. The extent of strand scission was quantified by calculating the nuclear diffusion factor, which represents the ratio between the total area of the halo plus nucleus and that of the nucleus. Data are expressed as relative nuclear diffusion factor, calculated by subtracting the nuclear diffusion factor of control cells from that of treated cells.

Statistical Analysis

Data from three independent experiments were used for evaluation of dose-response curves. IC_{50} values, expressed as mean of three independent determinations (±SD), were calculated by fitting the experimental data with a hyperbolic function and constraining Y_{max} to 100 (GraphPad Prism 4.00; GraphPad Software). Nonlinear regression R^2 values were >0.80 (Fig. 1C) or >0.95 (Fig. 2A).

Statistical significance of differences among data was estimated, unless differently stated, by two-tailed Student's *t* test.

Results

Inhibition of EGFR Autophosphorylation

UPR1024, a 1,5-disubstituted hydantoin (Fig. 1A), is a new compound previously characterized as an inhibitor of EGFR autophosphorylation in A431 cells (13). We analyzed the effect of UPR1024 on the level of EGFR autophosphorylation in the A549 lung cancer cell line by Western blotting. UPR1024 inhibited the EGF-induced EGFR autophosphorylation in a dose-dependent manner with an IC_{50} of 19.58 ± 6.02 μmol/L (Fig. 1B and C).

To test whether UPR1024 induced reversible or irreversible inhibition, cells were treated with the inhibitor (50 μmol/L) for 1 h and then washed free of drug. After 8 h, EGF was added for 5 min and EGFR autophosphorylation was determined. UPR1024 inhibition was completely reversible because phosphorylation was recovered after drug removal.

Inhibition of Cell Proliferation

We tested the antiproliferative effect of UPR1024 on a panel of NSCLC cell lines previously characterized in our laboratory for sensitivity to gefitinib.

After 72 h of treatment with 20 μmol/L UPR1024, all the cell lines tested showed a significant inhibition of cell proliferation (>40%; Fig. 1D) despite a very different sensitivity to gefitinib as indicated in the caption of the figure. UPR1024 inhibited A549 colony formation in a dose-dependent manner as assessed by clonogenic assay with an IC_{50} of 20.17 ± 1.81 μmol/L (Fig. 2A). As indicated in

Fig. 2B, drug exposure up to 24 h, followed by recovery time, did not significantly affect colony formation ability. However, a significant growth inhibitory activity was retained after 48-h exposure to 40 μmol/L, suggesting that long exposure to the drug is required for the appearance of the antiproliferative effect.

UPR1024 was cytostatic up to 10 μmol/L; however, at higher doses, a cytotoxic effect was detectable with appearance of floating dead cells and Annexin V–FITC/propidium iodide–positive cells (Fig. 2C). This result is in agreement with that observed by Chang (21) on the same cell line treated with similar concentrations of ZD1839 (gefitinib). To determine the effect of UPR1024 on A549 cell cycle distribution, cells treated with 20 and 40 μmol/L for 24 and 48 h were analyzed by flow cytometry. As shown in Fig. 2D, UPR1024 caused an increase in the proportion of cells in S phase with a decrease in G_1 phase. By contrast to gefitinib that induced a G_1 arrest in NSCLC cell lines (21–24), UPR1024 induced S arrest of the cell cycle, suggesting a different or additive target of action. This result has also been confirmed by BrdUrd incorporation experiments (not shown). An apoptotic sub-G_1 peak was detected, confirming that growth inhibition was associated with the activation of apoptotic pathways.

Induction of Apoptosis

To investigate the involvement of apoptotic cell death in UPR1024-induced cytotoxicity, several known markers of apoptosis were evaluated.

As shown in Fig. 3A, the activation of caspase-3 was negligible until 6 h of treatment becoming activated after 16 h at 40 μmol/L. The maximal activity was detectable after 48 h for both concentrations of drug tested.

We then investigated the cleavage of caspase-3, caspase-8, and caspase-9 by Western blotting to define the apoptotic pathways involved (Fig. 3B). We showed that UPR1024 treatment was associated with the activation of all three caspases. These proapoptotic proteins were strongly cleaved from their inactive precursor forms into active fragments. In line with these observations, cytochrome *c* was detected in the cytoplasm (Fig. 3C) concomitant with a marked decrease in mitochondrial membrane potential (data not shown) as determined by MitoCapture assay kit.

Because the Fas signaling pathway is involved in gefitinib-mediated apoptosis (21, 25), we monitored Fas plasma membrane expression in our system. UPR1024 induced an increase in Fas protein expression on the cell surface (data not shown).

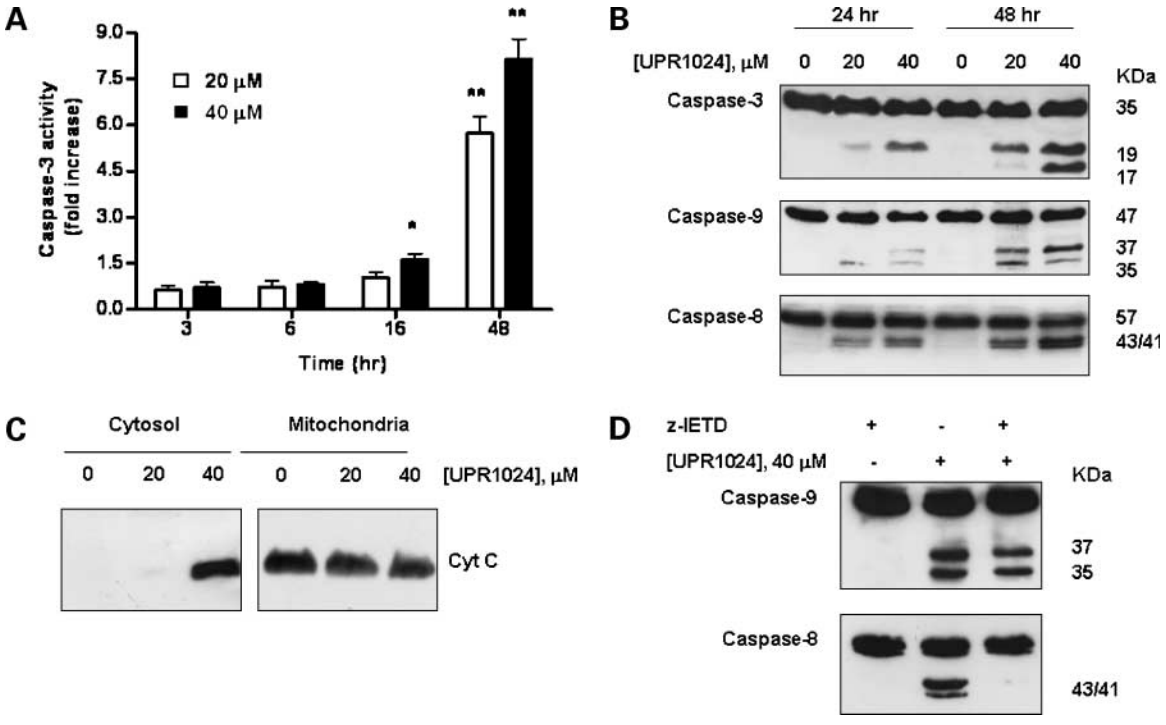

Figure 3. Caspase activation and cytochrome *c* release during UPR1024-induced apoptosis. **A,** caspase-3 activity was assessed in A549 cells exposed to 20 and 40 μmol/L UPR1024 for the indicated period of time. *Columns,* mean values of three independent experiments expressed as fold increase relative to control cells; *bars,* SD. One-tailed Student's *t* test; *, $P < 0.05$; **, $P < 0.01$; ***, $P < 0.001$ versus 1; $n = 3$. **B,** cleavage of procaspase-3, procaspase-8, and procaspase-9 was assessed on lysate proteins by Western blotting. The migration position of each full-length procaspase and of its processing products are indicated. **C,** cytochrome *c* release from mitochondria was assessed after 24 h of incubation by Western blot analysis of cell cytosolic and mitochondrial fractions. **D,** A549 cells were treated for 24 h in the absence or in the presence of 40 μmol/L caspase-8 inhibitor (z-IETD). Cleavage of procaspase-8 and procaspase-9 was assessed as in **B**. Results presented in **B**, **C**, and **D** are from representative experiments. Each experiment repeated twice yielded similar results.

As expected, the caspase-8 inhibitor z-IETD completely abolished cleavage of caspase-8 but did not prevent the cleavage of caspase-9 (Fig. 3D), indicating that caspase-9 activation was not a mere consequence of caspase-8 activity.

Taken together, these results indicated that intrinsic and extrinsic pathways are both involved in UPR1024-triggered apoptotic death in A549 cells.

Quantitation of DNA Damage

Taking into account the activation of the apoptotic intrinsic pathway induced by UPR1024 and considering that the α,β-unsaturated carbonyl fragment is featured by different cytotoxic agents that undergo interactions with DNA, we investigated the ability of the molecule to induce DNA damage. Fast halo assay was used to assess DNA damage in whole cells as previously reported (20). Control and UPR1024-treated cells were embedded in melted agarose spread onto microscope slides and lysed with a hypotonic solution at pH 13, which induced a radial diffusion from the nucleus of DNA fragments. Nuclei from A549 cells treated with 20 μmol/L UPR1024 for 3 h (Fig. 4A) showed a marked radial expansion (halo) of DNA fragments compared with nuclei from control cells. Quantitation of this effect, expressed as relative nuclear diffusion factor, is shown in Fig. 4B. Treatments with UPR1024 induced a concentration and time-dependent increase in the DNA damage, which reached a plateau at 16 h. Nuclear damage detected in cells treated with UPR1024 was not secondary to the onset of apoptosis as shown by the lack of caspase-3 activation until 16 h of treatment (see Fig. 3A).

As shown in Fig. 4C, UPR1024 induced DNA damage after 4 h of treatment that was completely repaired soon after withdrawal of the drug, suggesting a reversible effect on DNA.

p53 Accumulation

As shown by Western blot analysis, UPR1024 treatment induced p53 accumulation in A549 cells expressing wild-type p53 protein (Fig. 5A and B). The increase in the p53 level was evident after 16 h of treatment but not at earlier time points. $p21^{WAF1}$ protein level was detectable at 24 h and strongly increased after 48 h of treatment.

To determine whether the presence of p53 affects the biological effects of UPR1024, we used Calu-1 cells (a NSCLC cell line lacking p53) stably transfected with an ecdysone-inducible p53 expression vector. In this model, treatment with the inducer Ponasterone A caused a dose-dependent expression of p53 protein (14).

Calu-1 clones treated with 2.5 μmol/L Ponasterone A and 20 μmol/L UPR1024 showed higher levels of p53 in comparison with cells treated with Ponasterone A alone (Fig. 5C). Furthermore, additional Western blot analysis showed an Mdm2 down-regulation simultaneously with an increase in p53 in A549 treated with UPR1024 (data not shown), suggesting that Mdm2 down-regulation might be responsible for p53 accumulation.

p53 expression leads to $p21^{WAF1}$ up-regulation, and higher levels of the protein were observed in the presence of UPR1024.

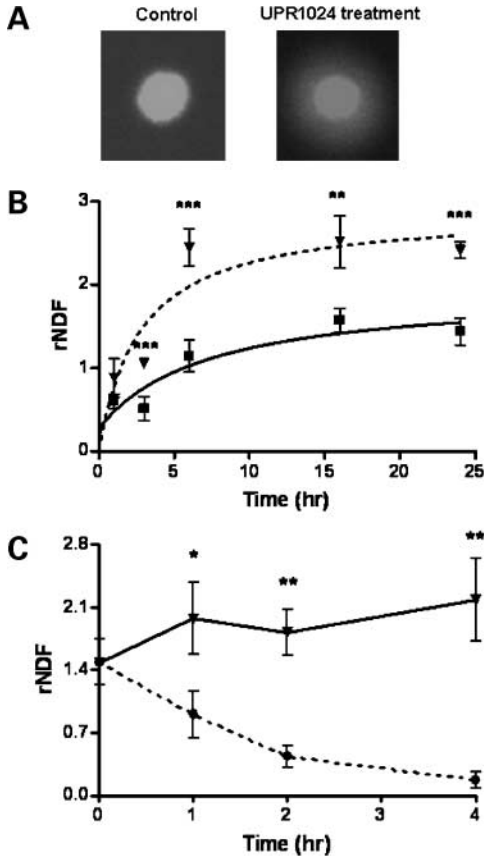

Figure 4. Quantitation of DNA damage. **A,** representative fast halo assay: images of nuclei from A549 cells untreated or treated with UPR1024 20 μmol/L for 3 h. **B,** A549 cells were incubated with UPR1024 at 20 (■) and 40 (▼) μmol/L for the indicated period of time or incubated (**C**) at 40 μmol/L for 4 h before a recovery period in a drug-free medium (●). Quantification of DNA damage was done by fast halo assay, as described in Materials and Methods. *Points,* mean values of three independent measurements; *bars,* SD. *, $P < 0.05$; **, $P < 0.01$; ***, $P < 0.001$ between doses (**B**) or 40 μmol/L versus drug-free medium (**C**) for the same period of time; $n = 3$-5.

Calu-1 clones were then analyzed for growth capability in the absence or in the presence of Ponasterone A and UPR1024 for 72 h.

As shown in Fig. 5D, in absence of Ponasterone A stimulation, cell number was significantly reduced only at 20 μmol/L UPR1024 treatment. Upon addition of the inducer (Ponasterone A), the number of Calu-1 cells reexpressing p53 treated with UPR1024 was reduced at lower concentration of the drug (1 μmol/L). It should be noted that the expression of p53 alone induced by 2.5 μmol/L Ponasterone A in the absence of UPR1024 significantly reduced cell proliferation (20% versus control).

Association between UPR1024 and Gefitinib

Taking into account that UPR1024 has a double target, we did an experiment designed to test whether UPR1024 treatment can overcome gefitinib resistance in SKLU-1 cells. As shown in Fig. 6A, gefitinib almost completely

inhibited EGFR autophosphorylation at 1 μmol/L without affecting cell proliferation (Fig. 6B), indicating that resistance mechanisms were activated to bypass EGFR inhibition. When UPR1024 was added to gefitinib, a significant inhibition in colony formation was observed (Fig. 6B), suggesting that UPR1024 is able to reduce proliferation even after the EGFR kinase activity was fully inhibited by gefitinib.

Discussion

Two main strategies for therapeutic targeting of EGFR have been developed: small-molecule inhibitors of the tyrosine kinase domain, such as gefitinib and erlotinib, and monoclonal antibodies, such as cetuximab, that are directed against the extracellular domain of EGFR and that inhibit phosphorylation and activation and stimulate internalization (26). In the case of gefitinib, survival improvement was found to be confined to certain patient subgroups (27). Investigations are in progress to identify molecular predictive markers of gefitinib responsiveness, such as EGFR mutations (7, 28, 29), EGFR gene copy number (30), and CA repeat polymorphism (31).

Tumor cells can develop several mechanisms that may result in resistance to gefitinib and erlotinib. Studies have revealed that additional oncogenic changes downstream of the EGFR (e.g., changes in the phosphatidylinositol 3′ kinase Akt pathway or K-ras) could also result in resistance to gefitinib and erlotinib (8). For this reason, new strategies for the simultaneous inhibition of multiple molecular targets are being pursued. One of these entails the combination of different molecular targets inhibitors (32).

The design and synthesis of new tyrosine kinase inhibitors is another rational approach to treat acquired resistance to erlotinib or gefitinib (33). The clinically available EGFR tyrosine kinase inhibitors belong to the chemical class of 4-aniloquinazolines, whose lack of structural diversity may lead to the appearance of cross-resistance and points to the need for novel molecules (34).

In a previous study, we examined the effect of a series of 1,5-disubstituted hydantoins on the inhibition of EGFR kinase activity and on cell growth. The results showed that UPR1024 is able to inhibit EGFR autophosphorylation and cell proliferation of A431 tumor cell line overexpressing EGFR protein (13).

In the present study, we confirmed our previous observations on a different cell model (NSCLC cell lines) showing that UPR1024 is capable of inhibiting EGF-induced EGFR autophosphorylation and cell proliferation leading to a preferential accumulation of cells in the S phase of the cell cycle. Moreover, new data on the biological effects of the molecule under investigation are presented, showing that UPR1024 has a second target at the DNA level.

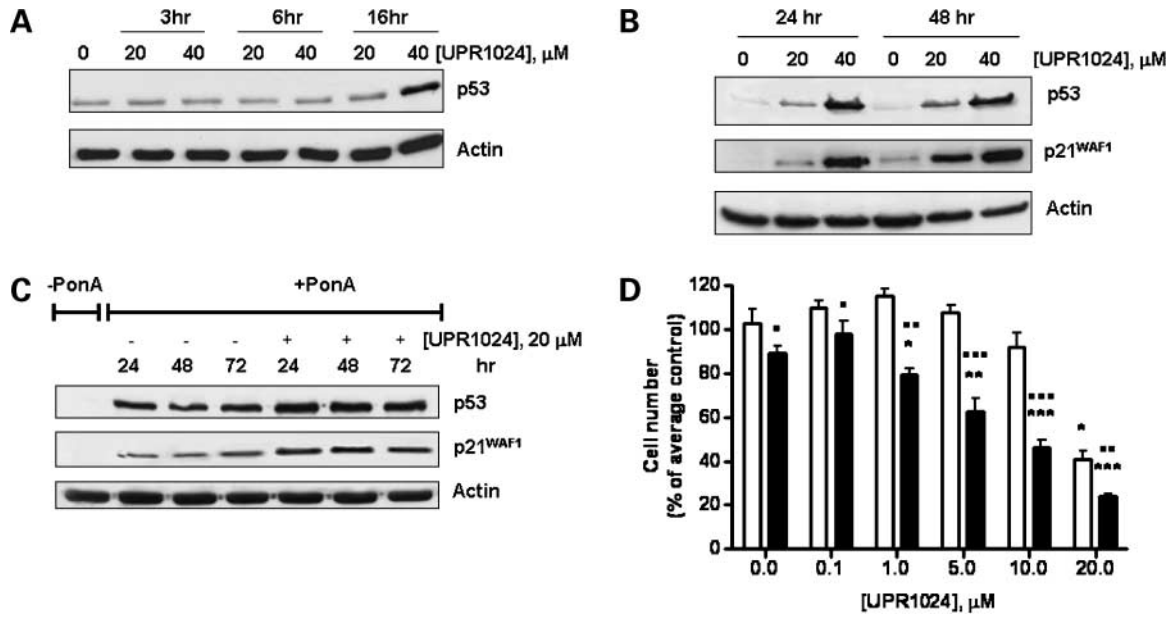

Figure 5. Modulation of p53 and $p21^{WAF1}$ protein expression during UPR1024 treatment and effect on cell proliferation. A549 cells were incubated with UPR1024 at the indicated concentration at early time points (**A**) or for 24 and 48 h (**B**). Cell lysates were analyzed by Western blotting to assess the expression of p53, $p21^{WAF1}$, and actin proteins. Representative blots of three independent experiments are shown. **C,** cells from Calu-1 inducible-p53 clone were incubated with 2.5 μmol/L Ponasterone A in the absence or in the presence of 20 μmol/L UPR1024 for the indicated period of time. Cell lysates were analyzed by Western blotting to assess the expression of p53 and $p21^{WAF1}$ proteins. Representative blots of three independent experiments. **D,** Calu-1 p53-expressing cell clone was treated with the indicated concentration of the drug in the absence (*empty columns*) or in the presence (*filled columns*) of 2.5 μmol/L Ponasterone A for 72 h. Results are presented as percentage of viable cells versus untreated control. *Columns,* mean values of three independent measurements; *bars,* SD. *, $P < 0.05$; **, $P < 0.01$; ***, $P < 0.001$ versus the corresponding control (UPR1024 absence); $n = 3$. ■, $P < 0.05$; ■■, $P < 0.01$; ■■■, $P < 0.001$ for each dose versus the corresponding untreated with Ponasterone A; $n = 3$.

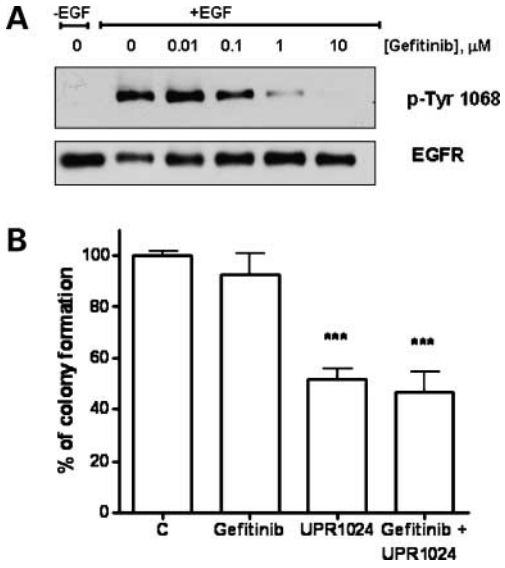

Figure 6. EGFR autophosphorylation and proliferation of SKLU-1 cell line exposed to gefitinib and/or UPR1024. **A,** SKLU-1 cells were serum starved for 16 h and then preincubated for 1 h with the indicated concentration of gefitinib before stimulation with 0.1 μg/mL EGF for 5 min. Western blot analysis was done by using monoclonal antibodies directed to p-Tyr^{1068} and to EGFR. **B,** cells were continuously exposed to 1 μmol/L gefitinib and/or 10 μmol/L UPR1024, and the ability of individual cell to form >50 cell colonies was assessed after 10 d. ***, $P < 0.001$ versus control; $n = 3$.

Treatment with gefitinib induced in A549 cancer cell line a G_1 arrest associated with up-regulation of p27 without any changes in p21^{WAF1} and p53 proteins (21, 25). Here, we show that in contrast to gefitinib, UPR1024 induced an S-phase growth arrest with up-regulation of p21^{WAF1} and p53. No p27 increase was observed in the same conditions. Moreover, we found that treatment with UPR1024 (at concentration of >10 μmol/L) for >24 h resulted in an apoptotic cell death as shown by externalization of phosphatidylserine, release of cytochrome *c*, appearance of DNA fragmentation, and activation of caspase-3, caspase-8, and caspase-9.

Hence, we show the involvement of both the extrinsic and intrinsic pathways in the UPR1024-mediated apoptosis, whereas activation of extrinsic apoptotic pathway depending on Fas seems to play a major role in the gefitinib-induced apoptosis (21, 25). Interestingly, increased Fas expression has been correlated with p53 translocation to the nucleus (25); however, modulation of p53 level in response to gefitinib has not been observed.

Treatment with UPR1024 induced a concentration-dependent and time-dependent increase in the DNA damage with a concomitant accumulation of p53 and p21^{WAF1}. It is known that DNA damage induces arrest in the cell cycle progression acting mainly in the G_1 phase, depending on the activation of the p53 and subsequently up-regulation of p21^{WAF1} (35). However, consistent with our results, treatment of the immortalized breast cell line MCF10A with topoisomerase I inhibitor SN38 (36) and treatment of human ovarian carcinoma cells with a new platinum (IV) complex (LA-12; ref. 37) induced an accumulation in S phase associated with the increased expression of p53 and p21^{WAF1}.

The role of p53 in the biological response to UPR1024 was evaluated in experiments involving reintroduction of p53 into a p53-negative lung cancer cell line (Calu-1).

Calu-1 cells, induced to express p53 treated with increased concentration of UPR1024, exhibited a more pronounced decrease in proliferation compared with cells not expressing p53. The drug was effective also in p53-negative cell lines (Calu-1, H1299) suggesting that p53 is not required for the inhibitory effect. However, there was a significant increase in sensitivity to UPR1024 in p53-positive cell lines.

These data indicate that, apart from anti-EGFR tyrosine kinase activity, UPR1024 induces additional cytotoxic DNA damage, a mechanism of action that may result in a significant antiproliferative and proapoptotic activity in refractory tumors. This conclusion is strongly supported by the observation that, in a cell model in which gefitinib is unable to reduce cell proliferation although autophosphorylation of the receptor is inhibited, the concomitant addition of UPR 1024 markedly reduced the capability to form colonies.

In particular, the α,β-unsaturated carbonyl substructure of UPR1024 may be partially responsible for its antiproliferative activity toward A549 cells. The characteristic reactivity of the α,β-unsaturated carbonyl moiety toward bionucleophiles may be responsible for the observed DNA damage effect and S-phase cell cycle arrest.

In a previous study, the *exo*-cyclic, conjugated double bond (the O=C-C=CHPh moiety) was shown to be an essential structural requirement for the biological activity of UPR1024 (13). Compounds containing the α,β-unsaturated carbonyl system can form cyclic adducts with DNA bases (38, 39) or can act as Michael acceptors in the reaction with -SH or -NH groups of bionucleophiles (40, 41). In addition to covalent bond formation, α,β-unsaturated carbonyl compounds can deplete cellular glutathione and promote the generation of reactive oxygen species (42). Therefore, the α,β-unsaturated carbonyl structure is an important feature for the cytotoxic antitumor activity of a wide range of natural products, such as helenalin (43), tenulin (44), and acronycine derivatives (45).

Although a clear characterization of its mechanism of action at the molecular level is required for further development of this class of compounds, the present data show that UPR1024 may be considered a new combi-molecule and could be inserted in a novel tumor strategy termed combi-targeting associating two modes of action within a single molecule. This approach had been successfully exploited by Jean-Claude's group for the anilinoquinazoline derivatives carrying a chloroethylamino (ZR2002; ref. 46), a triazene (RB24; ref. 47), or a nitrosourea (JDA58; ref. 48) fragment, all combining EGFR inhibition and DNA damage. The cooperative effect on double targets might enable broader antitumor activity and improve

efficacy. Further investigations on UPR1024 or its derivatives should lead to the design of compounds circumventing resistance to classic tyrosine kinase inhibitors in the treatment of lung cancer.

Acknowledgments

We thank Prof. Prisco Mirandola for helpful discussion.

References

1. Hanahan D, Weinberg RA. The hallmarks of cancer. Cell 2000;100: 57 – 70.

2. Jorissen RN, Walker F, Pouliot N, Garrett TP, Ward CW, Burgess AW. Epidermal growth factor receptor: mechanisms of activation and signalling. Exp Cell Res 2003;284:31 – 53.

3. Suzuki S, Dobashi Y, Sakurai H, Nishikawa K, Hanawa M, Ooi A. Protein overexpression and gene amplification of epidermal growth factor receptor in nonsmall cell lung carcinomas. An immunohistochemical and fluorescence *in situ* hybridization study. Cancer 2005;103:1265 – 73.

4. Schlessinger J. Cell signaling by receptor tyrosine kinases. Cell 2000; 103:211 – 25.

5. Fry DW. Mechanism of action of erbB tyrosine kinase inhibitors. Exp Cell Res 2003;284:131 – 9.

6. Kobayashi S, Boggon TJ, Dayaram T, et al. EGFR mutation and resistance of non-small-cell lung cancer to gefitinib. N Engl J Med 2005; 352:786 – 92.

7. Pao W, Miller VA, Politi KA, et al. Acquired resistance of lung adenocarcinomas to gefitinib or erlotinib is associated with a second mutation in the EGFR kinase domain. PLoS Med 2005;2:e73.

8. Camp ER, Summy J, Bauer TW, Liu W, Gallick GE, Ellis LM. Molecular mechanisms of resistance to therapies targeting the epidermal growth factor receptor. Clin Cancer Res 2005;11:397 – 405.

9. Rubin BP, Duensing A. Mechanisms of resistance to small molecule kinase inhibition in the treatment of solid tumors. Lab Invest 2006;86: 981 – 6.

10. Bianco C, Tortora G, Bianco R, et al. Enhancement of antitumor activity of ionizing radiation by combined treatment with the selective epidermal growth factor receptor-tyrosine kinase inhibitor ZD1839 (Iressa). Clin Cancer Res 2002;8:3250 – 8.

11. Ciardiello F, Caputo R, Bianco R, et al. Antitumor effect and potentiation of cytotoxic drugs activity in human cancer cells by ZD-1839 (Iressa), an epidermal growth factor receptor-selective tyrosine kinase inhibitor. Clin Cancer Res 2000;6:2053 – 63.

12. Sirotnak FM, Zakowski MF, Miller VA, Scher HI, Kris MG. Efficacy of cytotoxic agents against human tumor xenografts is markedly enhanced by coadministration of ZD1839 (Iressa), an inhibitor of EGFR tyrosine kinase. Clin Cancer Res 2000;6:4885 – 92.

13. Carmi C, Cavazzoni A, Zuliani V, et al. 5-benzylidene-hydantoins as new EGFR inhibitors with antiproliferative activity. Bioorg Med Chem Lett 2006;16:4021 – 5.

14. Cavazzoni A, Galetti M, Fumarola C, et al. Effect of inducible FHIT and p53 expression in the Calu-1 lung cancer cell line. Cancer Lett 2007;246: 69 – 81.

15. Cavazzoni A, Petronini PG, Galetti M, et al. Dose-dependent effect of FHIT-inducible expression in Calu-1 lung cancer cell line. Oncogene 2004; 23:8439 – 46.

16. Bradford MM. A rapid and sensitive method for the quantitation of microgram quantities of protein utilizing the principle of protein-dye binding. Anal Biochem 1976;72:248 – 54.

17. Adrain C, Creagh EM, Martin SJ. Apoptosis-associated release of Smac/DIABLO from mitochondria requires active caspases and is blocked by Bcl-2. EMBO J 2001;20:6627 – 36.

18. Fumarola C, La Monica S, Alfieri RR, Borra E, Guidotti GG. Cell size reduction induced by inhibition of the mTOR/S6K-signaling pathway protects Jurkat cells from apoptosis. Cell Death Differ 2005;12: 1344 – 57.

19. Fumarola C, La Monica S, Guidotti GG. Amino acid signaling through the mammalian target of rapamycin (mTOR) pathway: role of glutamine and of cell shrinkage. J Cell Physiol 2005;204:155 – 65.

20. Sestili P, Martinelli C, Stocchi V. The fast halo assay: an improved method to quantify genomic DNA strand breakage at the single cell level. Mutat Res 2006;607:205 – 14.

21. Chang GC, Hsu SL, Tsai JR, et al. Molecular mechanisms of ZD1839-induced G_1-cell cycle arrest and apoptosis in human lung adenocarcinoma A549 cells. Biochem Pharmacol 2004;68:1453 – 64.

22. Suenaga M, Yamaguchi A, Soda H, et al. Antiproliferative effects of gefitinib are associated with suppression of E2F-1 expression and telomerase activity. Anticancer Res 2006;26:3387 – 91.

23. Hotta K, Tabata M, Kiura K, et al. Gefitinib induces premature senescence in non-small cell lung cancer cells with or without EGFR gene mutation. Oncol Rep 2007;17:313 – 7.

24. Hirata A, Hosoi F, Miyagawa M, et al. HER2 overexpression increases sensitivity to gefitinib, an epidermal growth factor receptor tyrosine kinase inhibitor, through inhibition of HER2/HER3 heterodimer formation in lung cancer cells. Cancer Res 2005;65:4253 – 60.

25. Rho JK, Choi YJ, Ryoo BY, et al. p53 enhances gefitinib-induced growth inhibition and apoptosis by regulation of Fas in non-small cell lung cancer. Cancer Res 2007;67:1163 – 9.

26. Bunn PA, Jr., Franklin W. Epidermal growth factor receptor expression, signal pathway, and inhibitors in non-small cell lung cancer. Semin Oncol 2002;29:38 – 44.

27. Thatcher N, Chang A, Parikh P, et al. Gefitinib plus best supportive care in previously treated patients with refractory advanced non-small-cell lung cancer: results from a randomised, placebo-controlled, multicentre study (Iressa Survival Evaluation in Lung Cancer). Lancet 2005;366:1527 – 37.

28. Paez JG, Janne PA, Lee JC, et al. EGFR mutations in lung cancer: correlation with clinical response to gefitinib therapy. Science 2004;304: 1497 – 500.

29. Lynch TJ, Bell DW, Sordella R, et al. Activating mutations in the epidermal growth factor receptor underlying responsiveness of non-small-cell lung cancer to gefitinib. N Engl J Med 2004;350:2129 – 39.

30. Cappuzzo F, Hirsch FR, Rossi E, et al. Epidermal growth factor receptor gene and protein and gefitinib sensitivity in non-small-cell lung cancer. J Natl Cancer Inst 2005;97:643 – 55.

31. Han SW, Jeon YK, Lee KH, et al. Intron 1 CA dinucleotide repeat polymorphism and mutations of epidermal growth factor receptor and gefitinib responsiveness in non-small-cell lung cancer. Pharmacogenet Genom 2007;17:313 – 9.

32. Papaetis GS, Roussos C, Syrigos KN. Targeted therapies for non-small cell lung cancer. Curr Pharm Des 2007;13:2810 – 31.

33. Fry DW, Bridges AJ, Denny WA, et al. Specific, irreversible inactivation of the epidermal growth factor receptor and erbB2, by a new class of tyrosine kinase inhibitor. Proc Natl Acad Sci U S A 1998;95: 12022 – 7.

34. Kwak EL, Sordella R, Bell DW, et al. Irreversible inhibitors of the EGF receptor may circumvent acquired resistance to gefitinib. Proc Natl Acad Sci U S A 2005;102:7665 – 70.

35. Pucci B, Kasten M, Giordano A. Cell cycle and apoptosis. Neoplasia 2000;2:291 – 9.

36. Levesque AA, Kohn EA, Bresnick E, Eastman A. Distinct roles for p53 transactivation and repression in preventing UCN-01-mediated abrogation of DNA damage-induced arrest at S and G_2 cell cycle checkpoints. Oncogene 2005;24:3786 – 96.

37. Horvath V, Soucek K, Svihalkova-Sindlerova L, et al. Different cell cycle modulation following treatment of human ovarian carcinoma cells with a new platinum(IV) complex vs cisplatin. Invest New Drugs 2007;25: 435 – 43.

38. Eder E, Hoffman C, Bastian H, Deininger C, Scheckenbach S. Molecular mechanisms of DNA damage initiated by α, β-unsaturated carbonyl compounds as criteria for genotoxicity and mutagenicity. Environ Health Perspect 1990;88:99 – 106.

39. Freccero M, Di Valentin C, Sarzi-Amade M. Modeling H-bonding and solvent effects in the alkylation of pyrimidine bases by a prototype quinone methide: a DFT study. J Am Chem Soc 2003;125:3544 – 53.

40. Janecki T, Blaszczyk E, Studzian K, Janecka A, Krajewska U, Rozalski M. Novel synthesis, cytotoxic evaluation, and structure-activity relationship studies of a series of α-alkylidene-γ-lactones and lactams. J Med Chem 2005;48:3516 – 21.

41. Gonzalez AG, Silva MH, Padron JI, et al. Synthesis and antiproliferative activity of a new compound containing an α-methylene-γ-lactone group. J Med Chem 2002;45:2358 – 61.

42. Sathishkumar K, Rangan V, Gao X, Uppu RM. Methyl vinyl ketone induces apoptosis in murine GT1–7 hypothalamic neurons through glutathione depletion and the generation of reactive oxygen species. Free Radic Res 2007;41:469–77.

43. Lee KH, Hall IH, Mar EC, et al. Sesquiterpene antitumor agents: inhibitors of cellular metabolism. Science 1977;196:533–6.

44. Waddell TG, Austin AM, Cochran JW, Gerhart KG, Hall IH, Lee KH. Antitumor agents: structure-activity relationships in tenulin series. J Pharm Sci 1979;68:715–8.

45. David-Cordonnier MH, Laine W, Lansiaux A, et al. Alkylation of guanine in DNA by S23906–1, a novel potent antitumor compound derived from the plant alkaloid acronycine. Biochemistry 2002;41:9911–20.

46. Brahimi F, Rachid Z, Qiu Q, et al. Multiple mechanisms of action of ZR2002 in human breast cancer cells: a novel combi-molecule designed to block signaling mediated by the ERB family of oncogenes and to damage genomic DNA. Int J Cancer 2004;112:484–91.

47. Banerjee R, Rachid Z, Qiu Q, McNamee JP, Tari AM, Jean-Claude BJ. Sustained antiproliferative mechanisms by RB24, a targeted precursor of multiple inhibitors of epidermal growth factor receptor and a DNA alkylating agent in the A431 epidermal carcinoma of the vulva cell line. Br J Cancer 2004;91:1066–73.

48. Qiu Q, Domarkas J, Banerjee R, et al. The combi-targeting concept: *in vitro* and *in vivo* fragmentation of a stable combi-nitrosourea engineered to interact with the epidermal growth factor receptor while remaining DNA reactive. Clin Cancer Res 2007;13:331–40.